SCIENTIFIC REPORTS

OPEN

SUBJECT AREAS:
NANOPARTICLES
SYNTHESIS AND PROCESSING
ELECTROCATALYSIS
ELECTROCHEMISTRY

Received
14 May 2013

Accepted
3 July 2013

Published
22 July 2013

Correspondence and requests for materials should be addressed to G.X.W. (Guoxiu.Wang@uts.edu.au)

Ruthenium nanocrystals as cathode catalysts for lithium-oxygen batteries with a superior performance

Bing Sun[1], Paul Munroe[2] & Guoxiu Wang[1]

[1]Centre for Clean Energy Technology, School of Chemistry and Forensic Science, University of Technology Sydney, Broadway, Sydney, NSW 2007, Australia, [2]Electron Microscope Unit, The University of New South Wales, Sydney, NSW 2052, Australia.

The key factor to improve the electrochemical performance of Li-O_2 batteries is to find effective cathode catalysts to promote the oxygen reduction and oxygen evolution reactions. Herein, we report the synthesis of an effective cathode catalyst of ruthenium nanocrystals supported on carbon black substrate by a surfactant assisting method. The as-prepared ruthenium nanocrystals exhibited an excellent catalytic activity as cathodes in Li-O_2 batteries with a high reversible capacity of about 9,800 mAh g^{-1}, a low charge-discharge over-potential (about 0.37 V), and an outstanding cycle performance up to 150 cycles (with a curtaining capacity of 1,000 mAh g^{-1}). The electrochemical testing shows that ruthenium nanocrystals can significantly reduce the charge potential comparing to carbon black catalysts, which demonstrated that ruthenium based nanomaterials could be effective cathode catalysts for high performance lithium- O_2 batteries.

Rechargeable Li-O_2 batteries have been considered as the most advanced battery system to meet today's stringent requirements as the power source for electric vehicles. The energy density of Li-O_2 battery can reach up to 2–3 kWh kg^{-1}, which is the highest among all current rechargeable battery systems and compatible with gasoline[1–3]. However, the performances of Li-O_2 batteries are still constrained by several serious issues, including high charge-discharge over-potential, low rate capability, and poor cycling stability[4,5]. Furthermore, the energy efficiency of Li-O_2 batteries is much lower than current rechargeable non-aqueous and aqueous lithium batteries[2,6].

A typical rechargeable Li-O_2 battery consists of a porous air electrode as the cathode, a lithium metal as the anode and a nonaqueous Li^+ conducting electrolyte, in which the oxygen is drawn from the outside atmosphere and reduced by lithium ions from the electrolyte to form Li_2O_2 during the discharge process. During the charge process, the discharge products electrochemically decompose to lithium ions and oxygen[7–11]. However, the intermediate species of oxygen reduction reaction - lithium superoxide is a highly reactive base and can react with the commonly used organic carbonate-based electrolyte to form significant amount of lithium carbonates and lithium alkyl-carbonates[9,12,13]. Early studies of nonaqueous rechargeable Li-O_2 batteries based on these electrolytes only showed a few cycles with extremely high charge-discharge voltage gap and poor cycling stability[14,15]. Later, several investigations demonstrated that ether based electrolyte is more stable than carbonate based electrolyte[16]. However, it still suffers from increasing electrolyte decomposition upon cycling[17]. Recently, a novel dimethyl sulfoxide (DMSO) based electrolyte has been employed for Li-O_2 batteries and exhibited a high performance due to its remarkable stability against superoxides, good oxygen diffusion, high Li^+ conductivity, low volatility, and low viscosity[18]. Peng *et al.* demonstrated that it was possible to achieve 95% capacity retention after 100 cycles with the use of a DMSO electrolyte and a porous gold electrode[19]. The presence of Li_2O_2 corroborated by Fourier transform infrared (FTIR) spectroscopy and *in situ* surface-enhanced Raman spectroscopy (SERS) after many cycles demonstrated that DMSO based electrolyte should be suitable for rechargeable Li-O_2 batteries.

Another challenge for rechargeable Li-O_2 batteries is to reduce the large charge-discharge voltage gap to increase the electrical energy efficiency. Since the lithium anode has very little polarization, the large over-potential during charge-discharge is mainly caused by the sluggish oxygen reduction reaction (ORR) and oxygen evolution reaction (OER) of the air cathode. Although the widely used carbons themselves can act as good catalysts for ORR, they are not effective enough for the OER[20–25]. Furthermore, carbon materials always promote electrolyte decomposition to form Li_2CO_3 and lithium carboxylates[26–28]. Tremendous efforts have been devoted to

explore various cathode catalysts to address the above challenges, such as metal oxides, metal nitrides and precious metals[29–33]. Early investigation of cathode catalysts, including MnO_2 nanowires and PtAu alloy catalysts, were conducted using carbonate electrolyte[34–36]. Recently, bismuth and lead ruthenate pyrochlores, metallic mesoporous pyrochlore catalyst, Co_3O_4 grown on reduced graphene oxide, hydrate ruthenium oxide ($RuO_2 \cdot 0.6\ H_2O$) graphene oxide gel and perovskite porous $La_{0.75}Sr_{0.25}MnO_3$ nanotubes were reported in Li-O_2 cells with a glyme-based electrolyte and showed a high reversible capacity with a lower charge potential for OER than pure carbon[37–42]. The pure nanoporous gold as the electrode without any carbon or other additives demonstrated a lower over-potential and fast charge-discharge rate with the use of a DMSO electrolyte[19].

We developed an efficient cathode catalyst of ruthenium nanocrystals supported on carbon black (Ru-CB) by a surfactant assisting method. The as-prepared catalyst showed an excellent catalytic activity for ORR/OER in Li-O_2 batteries with a high reversible capacity and low charge-discharge over-potential (about 0.37 V). To our knowledge, this is the first report on Li-O_2 batteries with such low charge-discharge over-potential and high electrical energy efficiency. This research demonstrated that ruthenium nanocrystals could be a promising cathode catalyst for high performance Li-O_2 batteries.

Results

Synthesis and structural characterization of Ru-CB catalysts. The catalysts of ruthenium nanocrystals supported on carbon black were synthesized by a soft template methods followed by low temperature heat treatment. Fig. 1a. shows the schematic of the synthesis process. The typical synthesis process involved in the absorption of hydrophilic and hydrophobic tri-block copolymer F127 on the surface of carbon black nanoparticles to form homogeneous dispersion by ultrasonication and vigorous stirring. Then $RuCl_3$ was added with additional stirring for 24 h. During this process, ruthenium ions were absorbed on the long chain of the tri-block copolymer through weak coordination bonds between alkylene oxide segments and metal ions[43]. The final product was obtained by heat treatment of the as-prepared gel in a reducing atmosphere. The ruthenium content in Ru-CB nanocomposites was determined to be 34% calculated through the TGA measurement (Supplementary Fig. S1). Fig. 1b shows the X-ray diffraction (XRD) pattern of Ru-CB catalysts, in

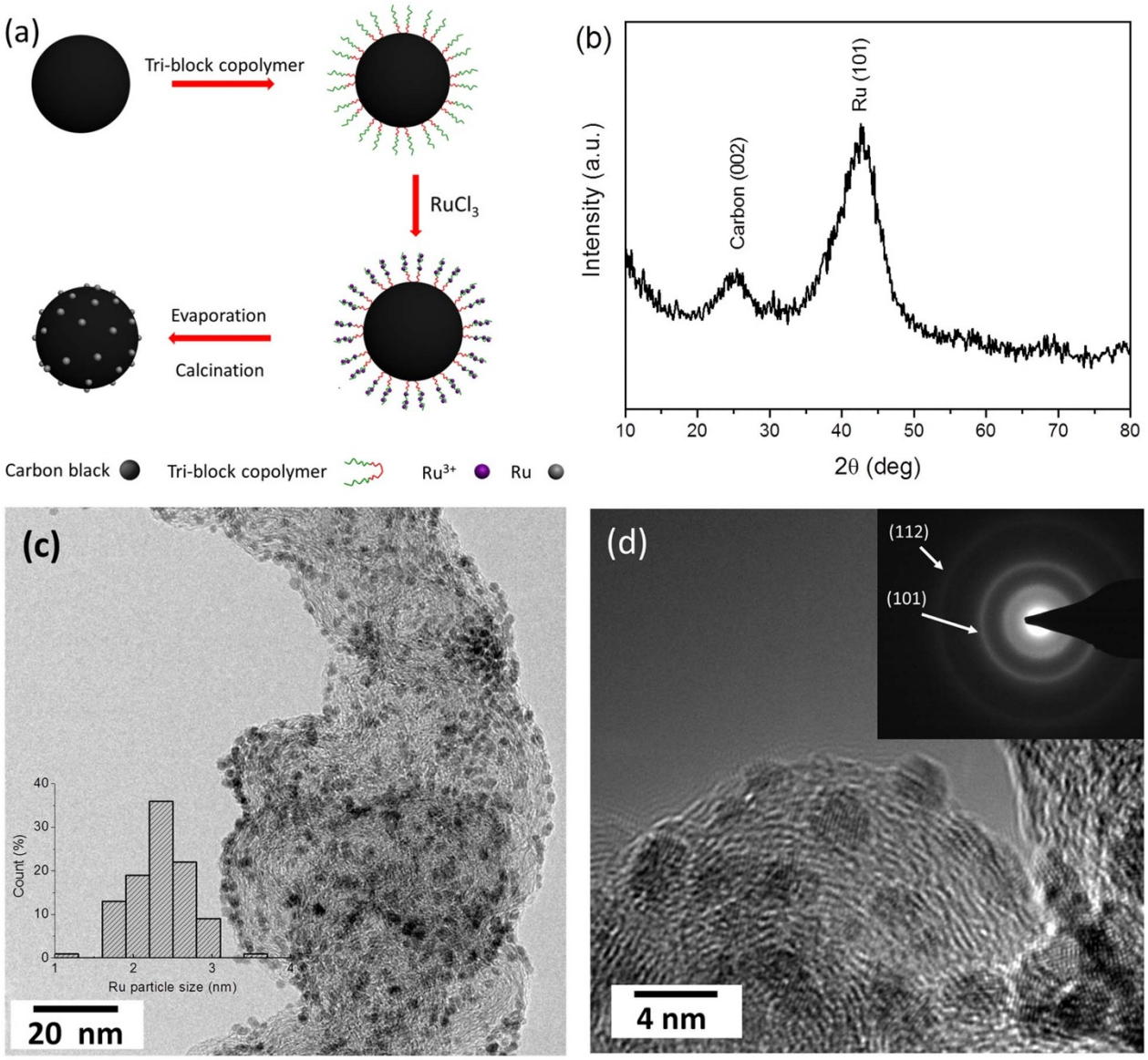

Figure 1 | Synthesis and structural characterization of Ru-CB catalysts. (a) Schematic illustration of the synthesis process of Ru-CB. (b) XRD pattern of Ru-CB. (c) TEM image and crystal size distribution of Ru nanocrystals. (d) High resolution TEM image of Ru-CB and the SAED pattern (inset).

which two main diffraction peaks can be indexed to carbon (002) and Ru(101). The transmission electron microscopy (TEM) shows that Ru nanocrystals are homogeneous distributed on the carbon black matrix with an average crystal size of 2.3 nm (Fig. 1c). Another low magnification TEM image in Supplementary Fig. S2 also shows the uniform distribution of Ru nanocrystals on carbon black matrix. High resolution TEM image further clearly demonstrates Ru nanocrystals anchored on the surface of carbon black (Fig. 1d).

Electrochemical performance of Ru-CB catalysts in Li-O_2 cells. The electrocatalytic activity of Ru-CB catalysts was examined in Li-O_2 cells and compared with bare carbon black (CB, Super-P). One key component in our Li-O_2 cell configuration is the oxygen diffusion electrode. The oxygen electrodes were made by coating the electrode materials on glass fiber separators, which allows efficient oxygen diffusion through the electrode (Supplementary Fig. S3). Another key factor in this experiment is the use of DMSO-based electrolyte because of the remarkable stability of DMSO against the formation of superoxides. Cyclic voltammetry (CV) was first employed to investigate the ORR and OER activity of the Ru-CB catalysts. The CV curves of Ru-CB and CB measured in the voltage range of 2.0–4.0 V are shown in Fig. 2a. Both Ru-CB and CB electrodes show a reduction peak during the cathodic scan, indicating the good catalytic activity of both Ru-CB and CB for ORRs. During the subsequent anodic scan process, strong oxidation (OER) peak can be observed at 3.9 V for Ru-CB electrode. The anodic peak intensity of the Ru-CB electrode is much higher than that of CB electrode, indicating the better catalytic activity of Ru-CB towards OER. In the second scan cycle, the CV curve of Ru-CB electrode shows a cathodic peak at 2.5 V with similar peak intensity as that in the first cycle. For the anodic scan process in the second cycle, the Ru-CB electrode still displays a strong oxidation peak at 3.7 V with the voltage even lower than that in the first cycle, demonstrating the good reversibility for ORR and OER. The anodic peak shifted from 3.9 V to 3.7 V, indicating that the electrode may undergo an electro-activation process[44]. However, there is only a small reduction peak appeared at 2.6 V in the second cathodic scan for the CV curves of the CB electrode, illustrating significant decrease of the catalytic activity. The CV measurement identified the much higher activity of Ru-CB catalysts for ORR and OER, comparing to bare carbon black catalysts.

The galvanostatic charge-discharge measurements were carried out to evaluate the electrochemical performances in the voltage range of 2.0–4.0 V for Ru-CB and 2.0–4.4 V for CB at room temperature. The background anodic scan results (Supplementary Fig. S4) demonstrated that DMSO based electrolyte is stable below 4.0 V for Ru-CB catalysts and is also stable below 4.2 V for CB catalysts, respectively. The typical charge-discharge voltage profiles are shown in Fig. 2b. The initial discharge capacity of the Ru-CB electrode is 9,800 mAh g^{-1}, which is significantly higher than the CB electrode (6,230 mAh g^{-1}). The discharge plateau of Ru-CB electrode is 2.8 V, which is also slightly higher than the CB electrode (2.76 V). For the charge process, significant differences were observed between Ru-CB electrode and CB electrode. The Ru-CB electrode shows much lower

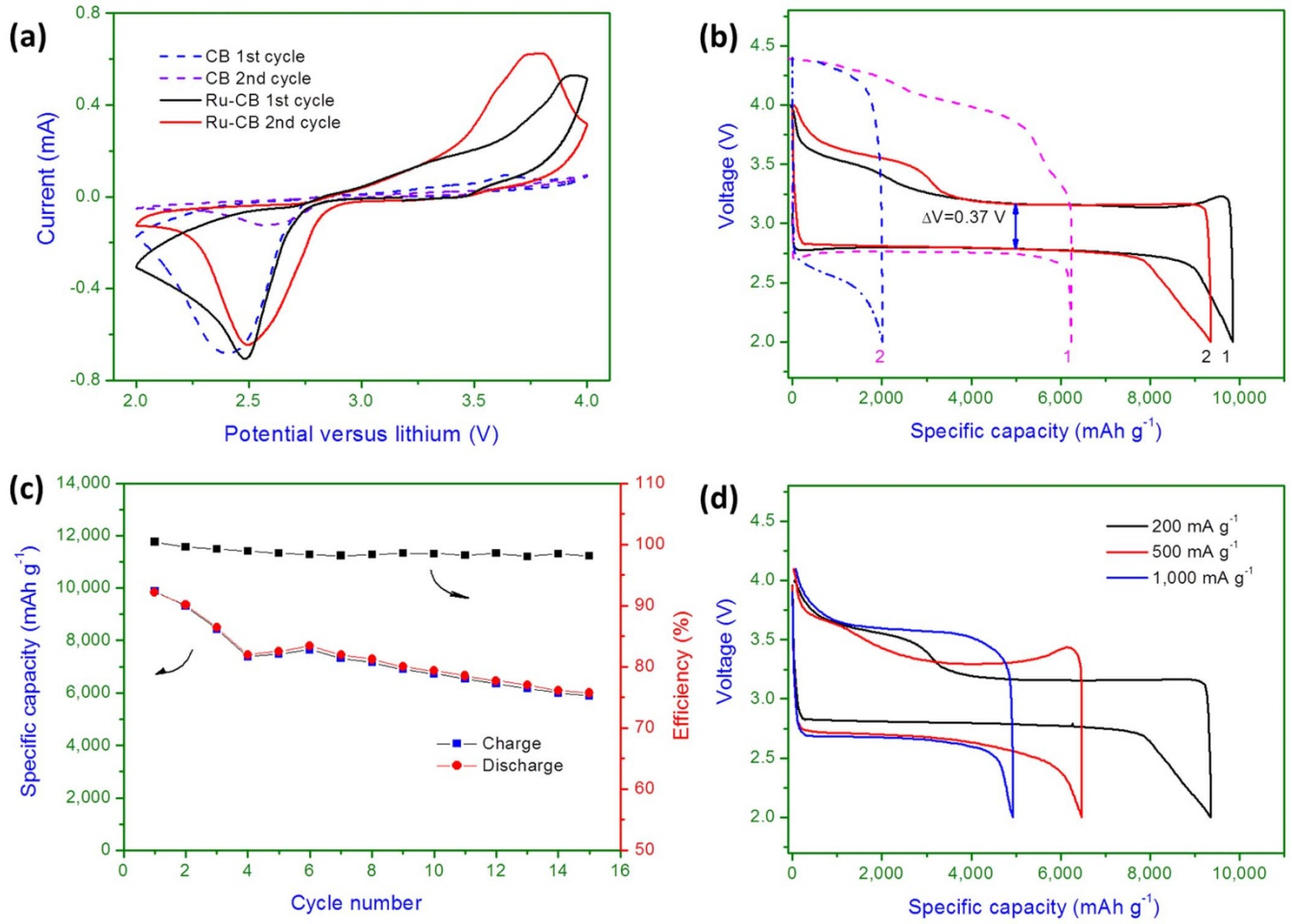

Figure 2 | Electrochemical characteristics for Ru-CB and CB catalysts in a Li-O_2 cell using a DMSO based electrolyte. (a) CV results at a constant scan rate of 0.05 mV s^{-1}. (b) Charge-discharge curves of the first two cycles for Ru-CB (solid line) and CB electrode (dash line) at 200 mA g^{-1}. (c) Cycling performance of Ru-CB at 200 mA g^{-1}. (d) The second cycle charge-discharge voltage curves of Ru-CB at different current densities.

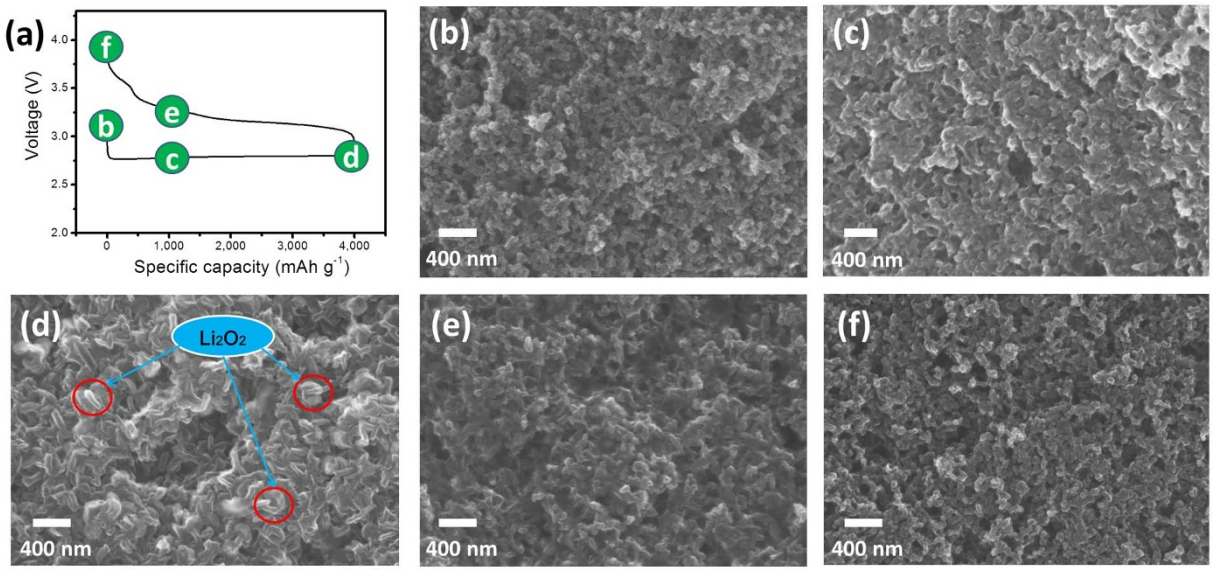

Figure 3 | Morphology observation of the Ru-CB electrodes at different states of discharge and charge. (a) Typical discharge-charge voltage profile of Ru-CB electrodes by curtailing the capacity to 4,000 mAh g^{-1}. (b-f) SEM images of Ru-CB electrodes taken at the points indicated in (a).

charge plateau than the CB electrode, illustrating excellent catalytic activity towards OER of Ru-CB catalysts. The main discharge products identified by *ex-situ* XRD (Supplementary Fig. S5) are Li_2O_2 and by-product LiOH. The first lower charge plateau (3.17 V) corresponds to the decomposition of Li_2O_2 and the second higher plateau could be associated with the decomposition of LiOH and other carbonate-based by-products. The charge potential of Ru-CB catalysts is also lower than the previously reported Ru-based catalysts, which may be owing to small particle size of discharge product Li_2O_2 and the use of novel DMSO-based electrolyte[32,39]. Furthermore, It should be noticed that 99.5% discharge capacity can be recharged below 4.0 V with a high energy efficiency of 83.37% and about 85% discharge capacity can be recharged below 3.5 V in the first cycle. Although the energy efficiency is slightly lower than the recently reported aqueous rechargeable lithium batteries (about 95%), the energy density of Li-O_2 cell with Ru-CB catalysts is much higher than the aqueous system. The discharge energy density of our Li-O_2 cells (Figure 2b) in the first cycle is 17,443 Wh kg^{-1} based on the total weight of the cathode electrode including Ru-CB catalysts and binder. This is much higher than other rechargeable lithium battery systems, including the recently reported aqueous lithium batteries (446 Wh kg^{-1})[6]. To the best of our knowledge, this is the first report that a Li-O_2 battery showed such low charge voltage plateau with a high specific capacity and high Coulombic efficiency. While for the CB electrode, most of the discharge capacity can only be recharged above 3.8 V in the first cycle. The cycling performance of the Ru-CB electrode is shown in Fig. 2c. Although the discharge capacity decreased upon cycling, the Ru-CB electrode still maintained a discharge capacity of 6,000 mAh g^{-1}, a high Coulombic efficiency of more than 98%, and relatively low charge-discharge over-potential in the 15th cycle (Supplementary Fig. S6).

The rate performance of Ru-CB catalysts was further investigated at higher charge-discharge current densities of 500 mA g^{-1} and 1000 mA g^{-1} between 2.0 and 4.1 V, respectively (Fig. 2d and Supplementary Fig. S7). The Ru-CB electrode delivered a discharge capacity of 6,500 mAh g^{-1} at 500 mA g^{-1} and more than 98% discharge capacity can be recharged under 4.1 V in the following charge process. When further increasing the current density to 1,000 mA g^{-1}, the Ru-CB electrode achieved a discharge capacity of 5,000 mAh g^{-1} in the second cycle. Even at high current density of 1,000 mA g^{-1}, the charge plateau of the Ru-CB electrode is still much lower than 4.0 V, which can avoid serious electrolyte decomposition at high voltage.

Discussion

The morphologies of the Ru-CB electrode at different states of discharge and charge were analyzed by FESEM (as shown in Fig. 3). After discharging the cell to 1,000 mAh g^{-1}, the Ru-CB electrode was covered with the discharge products. When we further discharge the cell to 4,000 mAh g^{-1}, large amount of toroid-like aggregates (Li_2O_2) were formed on the surface of the electrode (Fig. 3d). During the subsequent charge process, toroid-like Li_2O_2 disappeared at the charge capacity of 3,000 mAh g^{-1} (Fig. 3e). After charging the cell back to 4,000 mA g^{-1}, all discharge products completely disappeared (Fig. 3f), indicating the high reversibility of the Ru-CB electrode.

Catalytic activity of Ru-CB catalysts towards the oxygen evolution reaction. In order to confirm the catalytic activity of Ru-CB catalysts towards the oxidation of Li_2O_2, we did a slow anodic potential scan to investigate the OER behavior. The anodic scan experiments can avoid any morphological/compositional differences of the discharge products formed on the electrode during the discharge process[37]. Three kinds of electrodes with different composition were prepared with the first one containing CB only, the second one containing Li_2O_2/CB, and the third one composed of Li_2O_2/Ru-CB.

Figure 4a presents the anodic scan profiles for cells containing three different cathodes. The oxidation peak for the electrode containing Li_2O_2/Ru-CB occurs at 3.85 V, about 0.45 V lower than the electrode with Li_2O_2/CB, which the oxidation peak appeared at 4.3 V. The onset potential of the electrode with Ru-CB catalyst occurred at 3.3 V, which is also 0.5 V lower than the electrode with Li_2O_2/CB. The same electrode mixture without peroxide showed no oxidation peak features (Fig. 4a, blue dotted curve) except for the gradual onset of electrolyte decomposition at high voltage. Therefore, we verified that the OER is responsible for the oxidation current. We note that the position of the oxidation current peak for Ru-CB catalyst is similar to the anodic peaks of the Ru-CB electrode in Fig. 1a. Powder XRD data were also collected on the Li_2O_2/Ru-CB cathode before and after the anodic scan to 4.2 V and are presented in Fig. 4b. The results demonstrate that Li_2O_2 is completely absent at the end of the anodic scan. This further confirmed that Ru-CB catalysts have the capability to facilitate the OER of Li_2O_2 in Li-O_2 cells.

Improved cycling performance of Li-O_2 cells by the charge-discharge protocol of curtailing capacity. The cycling performance of Ru-CB catalysts was further examined by curtailing the

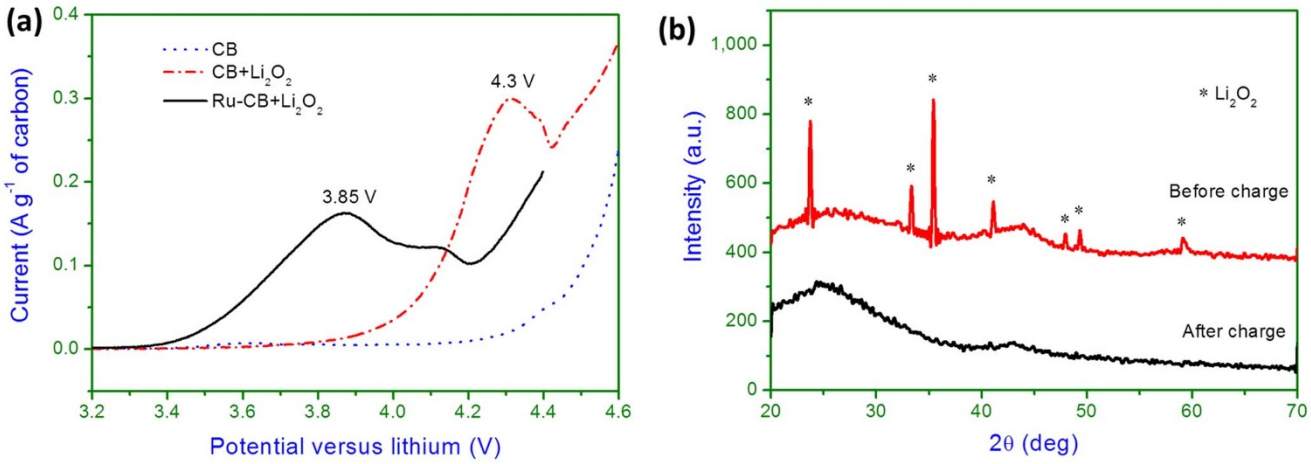

Figure 4 | Electrocatalytic oxidation of Li_2O_2 and XRD patterns of the electrode before and after the anodic scan. (a) Anodic scan profiles for electrocatalytic activity measurements of the Li_2O_2 oxidization by Ru-CB and CB catalysts at a scan rate of 0.02 mV s^{-1}. CB electrode without Li_2O_2 was used to collect the background profile. (b) *Ex situ* XRD patterns before and after an anodic potential scan to 4.2 V for the Ru-CB electrode. Crystalline Li_2O_2 was removed by oxidization.

capacity during cycling. Fig. 5a and b show the voltage profiles of Ru-CB electrodes cycled at 200 mA g^{-1} with the curtailing capacities of 1,000 mAh g^{-1} and 4,000 mAh g^{-1}, respectively. The Ru-CB catalysts display a discharge plateau at about 2.8 V and a charge plateau lower than 4.0 V for over 150 cycles. Even extending the curtailing capacity to 4000 mAh g^{-1}, the voltage profiles are still very stable. The cells showed a small over-potential about 0.365 V between charge and discharge, which is consistent with the result

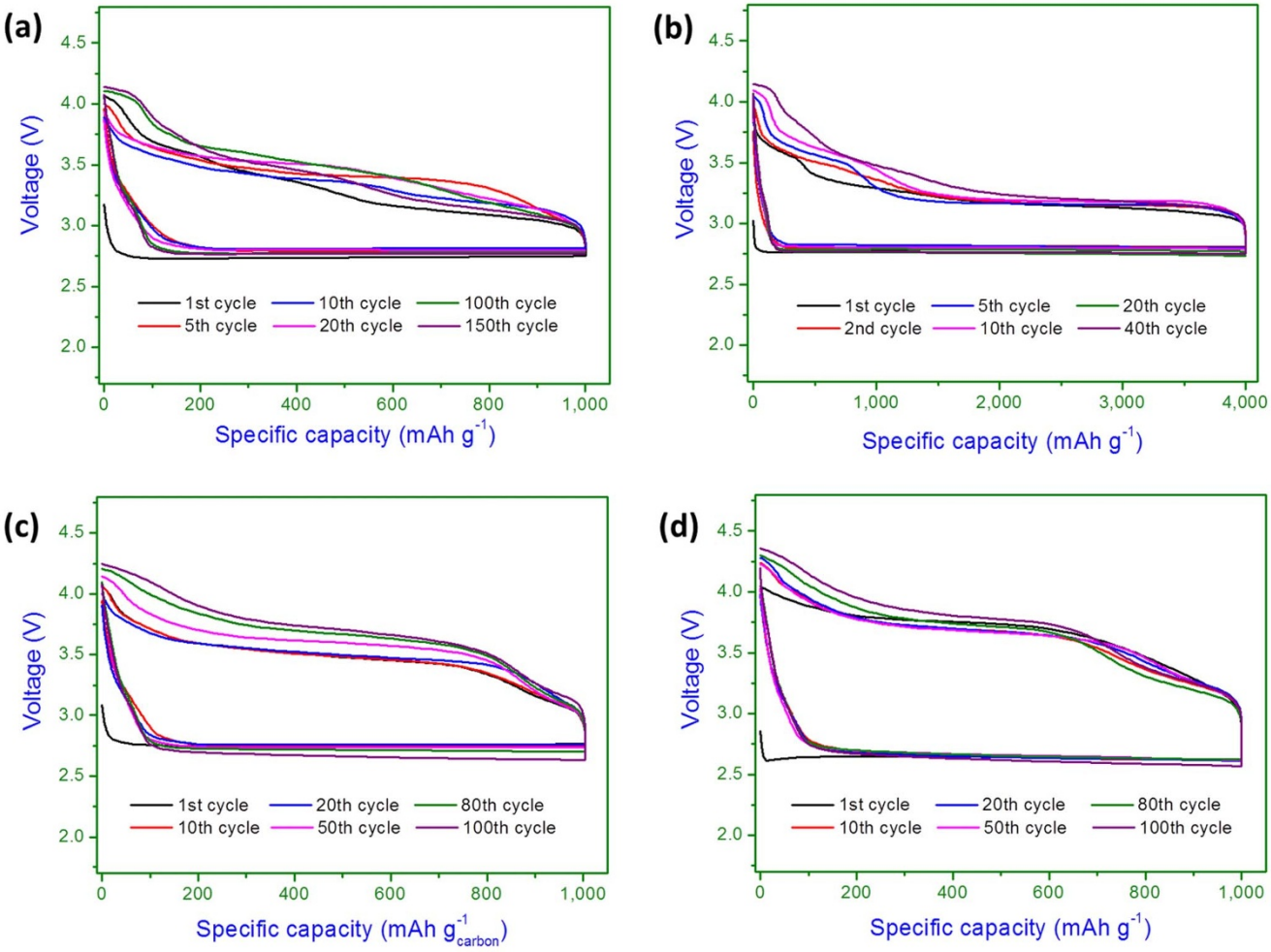

Figure 5 | Cycling performance of the Li-O_2 cells with Ru-CB catalyst at different capacity limits and current densities. (a,b) Voltage profiles of (a) 150 cycles at 200 mA g^{-1} with curtailing the capacity to 1,000 mAh g^{-1} and (b) 40 cycles at 200 mA g^{-1} with curtailing the capacity to 4,000 mAh g^{-1}. (c,d) Voltage profiles of 100 cycles at (c) 400 mA g^{-1} and (d) 1,000 mA g^{-1} with curtailing the capacity to 1,000 mAh g^{-1}.

shown in Fig. 1b (without curtailing capacity). No significant changes were observed for the cut-off voltages at each charge and discharge cycle (Supplementary Fig. S8a and S8b), demonstrating that the battery system is quite stable over many cycles. A comparison of voltage profiles between Li-O_2 cells with different charge-discharge capacity limitations are shown in Supplementary Fig. S9. As discharge capacity increased, more capacity can be recharged under 3.5 V with extended voltage plateau at 3.17 V. According to the FESEM observation results in Fig. 3, when we discharge the Ru-CB electrode to 4000 mAh g^{-1}, toroid-shaped Li_2O_2 were formed on the surface of the electrode. Therefore, Ru-CB catalysts can act as a promoter to enhance surface transport of Li_xO_2 species and efficiently catalyze the decomposition of toroid-shaped Li_2O_2 during the charging process (OER)[38].

The cycling tests were also performed by increasing the charge-discharge current densities to 400 mA g^{-1} and 1,000 mA g^{-1} (Fig. 5c and d). Both cells were cycled with a curtailing capacity of 1,000 mA g^{-1} for over 100 cycles. With the increase of current density, the charge-discharge voltage gap increased, owing to the increased ohmic polarization. However, there is no significant deterioration of the voltage profiles and the charge voltage plateau is still lower than 4.0 V. We also observed that there are no changes of the cut-off voltages for each charge and discharge cycle (Supplementary Fig. S8c and 8d). This implies that the Ru-CB catalysts can tolerate high charge-discharge current.

The above results demonstrate that Li-O_2 cells can operate reversibly with high efficiency, fast kinetics and good cycling stability. We believe that the much improved electrochemical performance should be ascribed to the Ru-CB catalysts combined with a stable electrolyte. DMSO-based electrolyte has been proved suitable for Li-O_2 batteries owing to its remarkable stability against superoxides, good oxygen diffusion ability, high Li^+ conductivity[18,19]. Our synthesized Ru-CB catalysts also showed much higher catalyst activity than that of bare carbon towards ORR and OER in Li-O_2 cells. Recently, it was reported that the nonaqueous Li^+ reduction reaction activity of Pd, Pt, Ru, Au and glassy carbon correlated to their surface oxygen adsorption energy. The oxygen adsorption energy on the surface can significantly influence the Li^+ oxygen reduction activities. The activity trend was found to be Pd > Pt >Ru ≈ Au> GC.[33] The oxygen adsorption energy on the surface of Ru is higher than carbon, which makes Ru more active towards the ORR than carbon black. Meanwhile, the Ru-CB catalysts are very stable during charge-discharge cycling. The morphologies of Ru-CB catalysts after charge-discharge for 50 cycles were observed by TEM. From the images in Supplementary Figure S10, we can see that there are no significant morphology changes after long term cycling. Recent report from Bruce's group clarified that carbon is stable below 3.5 V for both charge and discharge, but is unstable above 3.5 V in the charging process in the DMSO-based electrolyte[27]. The as-prepared Ru-CB catalysts can significantly reduce the charge potential to below 3.5 V. Therefore, the side reactions can be suppressed, leading to an enhanced electrochemical performance.

In summary, we report the achievement of high performance Li-O_2 batteries based on Ru nanocrystals catalysts that exhibited a high specific capacity of 9,800 mAh g^{-1} and an excellent cycle life. The Ru-CB catalysts were synthesized by a surfactant assisting method, in which Ru nanocrystals homogeneously distribute on carbon matrix. The Li-O_2 batteries show a low charge-discharge over-potential about 0.37 V. The Ru-CB catalysts also demonstrated superior cycle stability at different current densities up to 150 cycles at a curtailing capacity of 1,000 mAh g^{-1}. We also proved that Ru-CB catalysts can effectively decompose the discharge product – Li_2O_2, facilitating the OER, leading to a high round-trip efficiency. Therefore, Ru nanocrystals could be a promising cathode catalyst for rechargeable Li-O_2 batteries with superior performance.

Methods

Synthesis of Ru-CB catalysts. In a typical synthesis process, 24 mg carbon black (Super P) was firstly dispersed in 24 ml distilled water by ultrasonication for 10 min. Then 120 mg triblock copolymer $(HO(CH_2CH_2O)_{106}(CH_2CH(CH_3)O)_{70}(CH_2CH_2O)_{106}H)$ Pluronic® F127 was added under vigorous stirring for 24 h. Then, 0.8 ml $RuCl_3$ (20 mg ml^{-1} H_2O) was added to the above suspension under vigorous stirring for another 24 h. The resulting mixture was aged in air at 50 °C for 48 h in a Petri dish and then calcinated by heat treated at 300°C for 3 h under 5% H_2/Ar atmosphere.

Characterizations. X-ray diffraction pattern (XRD) measurement was conducted on a Siemens D5000 X-ray diffractionmeter using Cu Kα radiation. During the XRD analysis, the cathode electrodes with Li_2O_2 were enclosed with a thin transparent ploymer film to reduce their exposure to the ambient atmosphere. Field-emission scanning electron microscopy (FE-SEM, Zeiss Supra 55VP) and transmission electron microscopy (TEM, model JEM-2011, JEOL) were used to investigate the morphologies of the as-prepared samples and the air electrode before and after charge-discharge. Thermogravimetric analysis was carried out using a TA Instruments SDT 2960 at a heating rate of 10 °C min^{-1} in air.

Electrochemical testing of Li-O_2 cells. The oxygen electrodes were prepared as follows: Catalyst slurry was prepared by mixing the as-prepared catalysts (90 wt%) with poly(tetrafluoroethylene) (PTFE) (10 wt%) in isopropanol. The mixture was then coated on a glass fiber separator. The cathode film was punched into discs with a diameter of 14 mm and dried at 110 °C in a vacuum oven for 12 h. The typical loading of the air electrode is about 1 mg_{carbon} cm^{-2}. Swagelok type cell with an air hole (0.785 cm^2) on the cathode side was used to investigate the charge-discharge performance. The Li-O_2 cells were assembled in an Ar filled glove box (Mbraun) with water and oxygen level less than 0.1 ppm. A lithium foil was used as the anode and was separated by two glass microfibre filters, soaked in 0.1 M $LiClO_4$ (>99.99%, Aldrich) in dimethyl sulfoxide (DMSO, anhydrous, ≥ 99.9%, Sigma-Aldrich) electrolyte. The cell was gas-tight except for the stainless steel mesh window that exposed the porous cathode film to the oxygen atmosphere. All measurements were conducted in 1 atm dry oxygen atmosphere to avoid any negative effects of humidity and CO_2. Cyclic voltammogram were carried out on an electrochemical work station (CHI 660D) at a scan rate of 0.05 mV s^{-1} from 2.0 to 4.0 V. Galvanostatic discharge-charge was conducted on a Neware battery testing system. The specific capacity was calculated based on the mass of Super-P carbon black in the cathode electrodes. In the Li_2O_2 oxidation experiment, the electrodes containing Li_2O_2 were prepared inside the Ar filled glove box in the weight ratio of 1 : 1 : 2 (Li_2O_2 : Ru-CB/CB : binder). The electrodes without Li_2O_2 were prepared similarly with the weight ratio of 1 : 2 (CB : binder).

1. Bruce, P. G., Freunberger, S. A., Hardwick, L. J. & Tarascon, J. M. Li-O_2 and Li-S batteries with high energy storage. *Nat. Mater.* **11**, 19–29 (2012).
2. Girishkumar, G., McCloskey, B., Luntz, A. C., Swanson, S. & Wilcke, W. Lithium - Air Battery: Promise and Challenges. *J. Phys. Chem. Lett.* **1**, 2193–2203 (2010).
3. Lee, J. S. *et al.* Metal-Air Batteries with High Energy Density: Li-Air versus Zn-Air. *Adv. Energy Mater.* **1**, 34–50 (2011).
4. Christensen, J. *et al.* A Critical Review of Li/Air Batteries. *J. Electrochem. Soc.* **159**, R1–R30 (2012).
5. Li, F. J., Zhang, T. & Zhou, H. S. Challenges of non-aqueous Li-O_2 batteries: electrolytes, catalysts, and anodes. *Energy Environ. Sci.* **6**, 1125–1141 (2013).
6. Wang, X. J., Hou, Y. Y., Zhu, Y. S., Wu, Y. P. & Holze, R. An Aqueous Rechargeable Lithium Battery Using Coated Li Metal as Anode. *Sci. Rep.* **3** (2013).
7. Abraham, K. M. & Jiang, Z. A polymer electrolyte-based rechargeable lithium/oxygen battery. *J. Electrochem. Soc.* **143**, 1–5 (1996).
8. Ogasawara, T., Debart, A., Holzapfel, M., Novak, P. & Bruce, P. G. Rechargeable Li_2O_2 electrode for lithium batteries. *J. Am. Chem. Soc.* **128**, 1390–1393 (2006).
9. McCloskey, B. D., Bethune, D. S., Shelby, R. M., Girishkumar, G. & Luntz, A. C. Solvents' Critical Role in Nonaqueous Lithium-Oxygen Battery Electrochemistry. *J. Phys. Chem. Lett.* **2**, 1161–1166 (2011).
10. Jung, H. G. *et al.* A Transmission Electron Microscopy Study of the Electrochemical Process of Lithium-Oxygen Cells. *Nano Lett.* **12**, 4333–4335 (2012).
11. Peng, Z. Q. *et al.* Oxygen Reactions in a Non-Aqueous Li^+ Electrolyte. *Angew. Chem. Int. Ed.* **50**, 6351–6355 (2011).
12. Freunberger, S. A. *et al.* Reactions in the Rechargeable Lithium-O_2 Battery with Alkyl Carbonate Electrolytes. *J. Am. Chem. Soc.* **133**, 8040–8047 (2011).
13. Bryantsev, V. S. *et al.* Predicting Solvent Stability in Aprotic Electrolyte Li-Air Batteries: Nucleophilic Substitution by the Superoxide Anion Radical ($O_2^{\bullet-}$). *J. Phys. Chem. A* **115**, 12399–12409 (2011).
14. Sun, B., Liu, H., Munroe, P., Ahn, H. & Wang, G. X. Nanocomposites of CoO and a mesoporous carbon (CMK-3) as a high performance cathode catalyst for lithium-oxygen batteries. *Nano Res.* **5**, 460–469 (2012).
15. Zhang, L. L. *et al.* High aspect ratio gamma-MnOOH nanowires for high performance rechargeable nonaqueous lithium-oxygen batteries. *Chem. Commun.* **48**, 7598–7600 (2012).
16. Laoire, C. O., Mukerjee, S., Plichta, E. J., Hendrickson, M. A. & Abraham, K. M. Rechargeable Lithium/TEGDME-LiPF6/O_2 Battery. *J. Electrochem. Soc.* **158**, A302–A308 (2011).

17. Freunberger, S. A. *et al.* The Lithium-Oxygen Battery with Ether-Based Electrolytes. *Angew. Chem. Int. Ed.* **50**, 8609–8613 (2011).
18. Xu, D., Wang, Z. L., Xu, J. J., Zhang, L. L. & Zhang, X. B. Novel DMSO-based electrolyte for high performance rechargeable Li-O_2 batteries. *Chem. Commun.* **48**, 6948–6950 (2012).
19. Peng, Z. Q., Freunberger, S. A., Chen, Y. H. & Bruce, P. G. A Reversible and Higher-Rate Li-O_2 Battery. *Science* **337**, 563–566 (2012).
20. Laoire, C. O., Mukerjee, S., Abraham, K. M., Plichta, E. J. & Hendrickson, M. A. Elucidating the Mechanism of Oxygen Reduction for Lithium-Air Battery Applications. *J. Phys. Chem. C* **113**, 20127–20134 (2009).
21. Xiao, J. *et al.* Hierarchically Porous Graphene as a Lithium-Air Battery Electrode. *Nano Lett.* **11**, 5071–5078 (2011).
22. Li, Y. L. *et al.* Superior energy capacity of graphene nanosheets for a nonaqueous lithium-oxygen battery. *Chem. Commun.* **47**, 9438–9440 (2011).
23. Sun, B. *et al.* Graphene nanosheets as cathode catalysts for lithium-air batteries with an enhanced electrochemical performance. *Carbon* **50**, 727–733 (2012).
24. Beattie, S. D., Manolescu, D. M. & Blair, S. L. High-Capacity Lithium-Air Cathodes. *J. Electrochem. Soc.* **156**, A44–A47 (2009).
25. Mitchell, R. R., Gallant, B. M., Thompson, C. V. & Shao-Horn, Y. All-carbon-nanofiber electrodes for high-energy rechargeable Li-O_2 batteries. *Energy Environ. Sci.* **4**, 2952–2958 (2011).
26. Gallant, B. M. *et al.* Chemical and Morphological Changes of Li-O_2 Battery Electrodes upon Cycling. *J. Phys. Chem. C* **116**, 20800–20805 (2012).
27. Thotiyl, M. M. O., Freunberger, S. A., Peng, Z. Q. & Bruce, P. G. The Carbon Electrode in Nonaqueous Li-O_2 Cells. *J. Am. Chem. Soc.* **135**, 494–500 (2013).
28. McCloskey, B. D. *et al.* Twin Problems of Interfacial Carbonate Formation in Nonaqueous Li-O_2 Batteries. *J. Phys. Chem. Lett.* **3**, 997–1001 (2012).
29. Debart, A., Bao, J., Armstrong, G. & Bruce, P. G. An O_2 cathode for rechargeable lithium batteries: The effect of a catalyst. *J. Power Sources* **174**, 1177–1182 (2007).
30. Shao, Y. Y. *et al.* Electrocatalysts for Nonaqueous Lithium-Air Batteries: Status, Challenges, and Perspective. *Acs Catal.* **2**, 844–857 (2012).
31. Li, F. J. *et al.* Carbon supported TiN nanoparticles: an efficient bifunctional catalyst for non-aqueous Li-O_2 batteries. *Chem. Commun.* **49**, 1175–1177 (2013).
32. Harding, J. R., Lu, Y. C., Tsukada, Y. & Shao-Horn, Y. Evidence of catalyzed oxidation of Li_2O_2 for rechargeable Li-air battery applications. *Phys. Chem. Chem. Phys.* **14**, 10540–10546 (2012).
33. Lu, Y. C., Gasteiger, H. A. & Shao-Horn, Y. Catalytic Activity Trends of Oxygen Reduction Reaction for Nonaqueous Li-Air Batteries. *J. Am. Chem. Soc.* **133**, 19048–19051 (2011).
34. Debart, A., Paterson, A. J., Bao, J. & Bruce, P. G. alpha-MnO_2 nanowires: A catalyst for the O_2 electrode in rechargeable lithium batteries. *Angew. Chem. Int. Ed.* **47**, 4521–4524 (2008).
35. Lu, Y. C. *et al.* Platinum-Gold Nanoparticles: A Highly Active Bifunctional Electrocatalyst for Rechargeable Lithium-Air Batteries. *J. Am. Chem. Soc.* **132**, 12170–12171 (2010).
36. Lu, Y. C., Gasteiger, H. A., Parent, M. C., Chiloyan, V. & Shao-Horn, Y. The Influence of Catalysts on Discharge and Charge Voltages of Rechargeable Li-Oxygen Batteries. *Electrochem. Solid-State Lett.* **13**, A69–A72 (2010).
37. Oh, S. H., Black, R., Pomerantseva, E., Lee, J. H. & Nazar, L. F. Synthesis of a metallic mesoporous pyrochlore as a catalyst for lithium-O_2 batteries. *Nat. Chem.* **4**, 1004–1010 (2012).
38. Black, R., Lee, J. H., Adams, B., Mims, C. A. & Nazar, L. F. The Role of Catalysts and Peroxide Oxidation in Lithium-Oxygen Batteries. *Angew. Chem. Int. Ed.* **52**, 392–396 (2013).
39. Jung, H. G. *et al.* Ruthenium-Based Electrocatalysts Supported on Reduced Graphene Oxide for Lithium-Air Batteries. *Acs Nano* **7**, 3532–3539 (2013).
40. Oh, S. H. & Nazar, L. F. Oxide Catalysts for Rechargeable High-Capacity Li-O_2 Batteries. *Adv. Energy Mater.* **2**, 903–910 (2012).
41. Wang, Z. L., Xu, D., Xu, J. J., Zhang, L. L. & Zhang, X. B. Graphene Oxide Gel-Derived, Free-Standing, Hierarchically Porous Carbon for High-Capacity and High-Rate Rechargeable Li-O_2 Batteries. *Adv. Funct. Mater.* **22**, 3699–3705 (2012).
42. Xu, J. J. *et al.* Synthesis of Perovskite-Based Porous $La_{0.75}Sr_{0.25}MnO_3$ Nanotubes as a Highly Efficient Electrocatalyst for Rechargeable LithiumOxygen Batteries. *Angew. Chem. Int. Ed.* **52**, 3887–3890 (2013).
43. Yang, P. D., Zhao, D. Y., Margolese, D. I., Chmelka, B. F. & Stucky, G. D. Generalized syntheses of large-pore mesoporous metal oxides with semicrystalline frameworks. *Nature* **396**, 152–155 (1998).
44. Jung, H. G., Hassoun, J., Park, J. B., Sun, Y. K. & Scrosati, B. An improved high-performance lithium-air battery. *Nature Chem.* **4**, 579–585 (2012).

Acknowledgements

This project was financially supported by the Australian Research Council (ARC) through the ARC FT project (FT110100800).

Author contributions

B.S. performed the major part of the experiments. P.M. performed TEM characterisation. B.S. and G.-X.W. conceived the study and wrote the manuscript. All authors discussed the results on the manuscript.

Additional information

Supplementary Information accompanies this paper at http://www.nature.com/scientificreports

Competing financial interests: The authors declare no competing financial interests.

How to cite this article: Sun, B., Munroe, P. & Wang, G.X. Ruthenium nanocrystals as cathode catalysts for lithium-oxygen batteries with a superior performance. *Sci. Rep.* **3**, 2247; DOI:10.1038/srep02247 (2013).